Journal of Structural Geology, Vol. 9, No. 2, pp. 139 to 157, 1987
Printed in Great Britain

0191-8141/87 $03.00+0.00

The Palomares brittle–ductile Shear Zone of southern Spain

RUUD WEIJERMARS

The Hans Ramberg Tectonic Laboratory, Institute of Geology, Uppsala University, Box 555, S-751 22 Uppsala, Sweden

(*Received 2 December 1985; accepted in revised form 23 August 1986*)

Abstract—The Palomares Shear Zone is a major Neogene–Quaternary strike–slip zone which transects the crust of the Betic Cordillera in SE Spain. The shear zone and the mechanisms that led to its formation are discussed and illustrated on the basis of detailed compilations of both the local and regional geology. It is emphasized that the formation of the Palomares Shear Zone was not an isolated tectonic event, but part of a complex Neogene tectonic history. The Neogene evolution of the Betic-Rif orogen and its central Alboran Basin is characterised by the following events: (1) emplacement of the Alboran Diapir with resulting nappe-shedding from the overlying crust between 25 and 20 Ma ago; (2) onset of the subsidence of the Alboran Basin between 20 and 15 Ma ago due to cooling of the Alboran Diapir and the overlying crust; (3) formation of the Cabo de Gata Volcanic Chain between 15 and 8 Ma ago; and (4) refolding of the nappe sheets in the Betic-Rif orogen into a basin and range structure about 7 Ma ago. Continuous activity of the Crevillente Fault of southern Spain may have occurred over a period from 20 Ma ago up to the present. The interrelated Palomares Fault in SE Spain was probably formed between 15 and 8 Ma ago and seems to be active still. The Palomares Shear Zone affects a rock volume 44 km wide, at least 80 km long and 30 km deep. A shear strain–distance diagram constructed across the Palomares Shear Zone and its axial Palomares Fault involves a new method to estimate or constrain the shear strain magnitude along brittle–ductile shears. The typical tensor shear strain rates in the approximately 20 km thick ductilely deformed walls of the Palomares Fault are of the order 10^{-13}–10^{-14} s^{-1}. The tensor shear strain rate along the Palomares Fault itself is of the order 10^{-12} s^{-1} and the time averaged relative displacement rate of its walls is about 2 mm a^{-1}. The range of strain rates within the Palomares Shear Zone are interpreted to be due to a combination of various flow-softening mechanisms: geometric, structural, thermal and strain-rate softening. These softening mechanisms might explain the difference in vertically averaged viscosities of 10^{20} Pa s and 10^{25} Pa s or lower suggested for the crustal rocks in the Palomares Fault proper and that of the relatively rigid boundaries of the Palomares Shear Zone, respectively.

INTRODUCTION

THE ARC of Gibraltar is defined by two mountain belts: the Betic Cordilleras of southern Spain and the Rif Mountains of Morocco (Fig. 1). The Betic Cordilleras are normally subdivided into an External Zone in the north and an Internal (or Betic) Zone in the south (cf. Egeler & Simon 1969a,b). The External Zone is subdivided into Pre-Betic and Sub-Betic districts (Fig. 1), separated by a thrust zone. The thrusting of the Sub-Betic over the Pre-Betic occurred in Tortonian times (Jerez-Mir 1973, Hoedemaeker 1973, Azema 1977).

Only recently it has been recognised that part of the contact between the Sub-Betic and Pre-Betic is a major dextral strike–slip fault, the Crevillente Fault (Foucault 1971, Hermes 1978, Van de Fliert *et al.* 1980, De Smet 1984a,b) (Fig. 1). Deformation along the Crevillente Fault is characterised by the formation of a tectonic melange consisting of huge km-size allochthonous blocks and cataclasites with a geometry which in section has been termed a 'flower-structure' (De Smet 1984b). The main movements along the Crevillente Fault appear to have taken place during the Miocene between 20 and 5 Ma ago with a total displacement of approximately 250 km (Hermes 1978, De Smet 1984b).

The existence of other, possibly related, major wrench faults in the eastern Betic Cordilleras has been suggested since the 1960's (Fernex 1964, Rondeel 1965, Völk 1967, Westra 1969, Bousquet 1979), but detailed analyses have not yet been attempted. Wrench faulting can be shown to have been the last major tectonic event which affected the crust of SE Spain as the Neogene evolution of the Betic-Rif orogen and the central Alboran Basin drew to a close. The existence of such major wrench faults can be documented by detailed compilation of the geology of the eastern Betic Cordilleras.

GEOLOGICAL SETTING

The Alboran Sea, the western branch of the Mediterranean Sea enclosed by the Arc of Gibraltar, is presently connected with the Atlantic Ocean by the Strait of Gibraltar. However, it has been argued that a topographic high at the site of the Alboran Sea separated the Mediterranean Sea from the Atlantic Ocean until about 20 Ma ago (Weijermars 1985a,b). Inversion of the topographic high into a depression is considered to have occurred by cooling of the crust after thinning by a mantle diapir (Weijermars 1985b). The Alboran Basin is now filled with a 4–6 km thick Neogene succession (Mulder 1973, Mulder & Parry 1977) with a pronounced surface relief at an average depth of 1 km below sea level (Stanley *et al.* 1970). The presence of a mantle diapir beneath the Alboran Basin is suggested both by seismic reflection profiles (Banda *et al.* 1983, Marillier & Mueller 1985) and gravity anomalies (Hofman 1952, Van Bem-

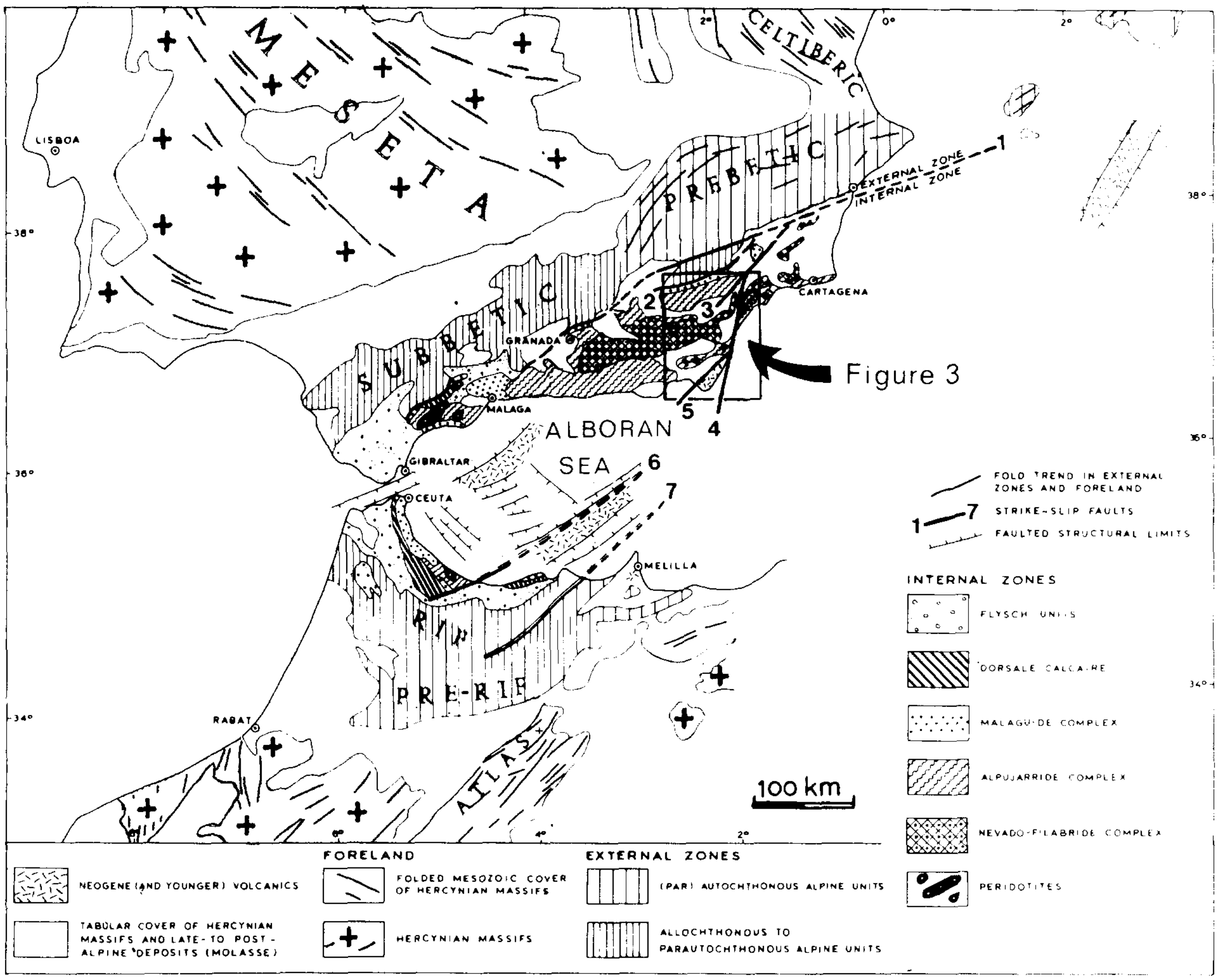

Fig. 1. Tectonic map of the Alboran Basin, Betic–Rif orogen, Atlas Mountains and the Spanish Meseta. Major lineaments are (1) Crevillente Fault, (2) Velez Rubio Corridor, (3) Alhama de Murcia Fault, (4) Palomares Fault, (5) Almería Fault Zone, (6) Jedha Fault and (7) Nekor Fault. (Compiled after Le Pichon *et al.* 1972, Araña & Vegas 1974, Kampschuur & Rondeel 1975, Hermes 1978, 1984, and Rondeel *et al.* 1984.) The outline of Fig. 3 is shown.

melen 1952, 1969, 1973, Bonini *et al.* 1973, Loomis 1975).

The Arc of Gibraltar or Betic-Rif orogen is commonly termed an Alpine fold belt, although all the major tectonic events occurred in Neogene times (Weijermars 1985a,b). The fold nappes in the Betic-Rif orogen are postulated to have formed by Late Oligocene nappe-shedding from the lithospheric bulge caused by the emplacement of the Alboran Diapir 25–20 Ma ago (Fig. 2a). The Late Oligocene nappes, some of which were emplaced under greenschist facies metamorphic conditions, were subsequently brought to the surface by isostatic recovery of downwarps at the base of the lithosphere peripheral to the Alboran Diapir (Fig. 2b) (Weijermars 1985b). The trend of the Neogene basin-and-range structure, which defines the morphology of the Betic Cordilleras, is due to the uplift and refolding of the nappes after their emplacement. Refolding of the SE part of the Betic Cordilleras occurred near the end of the Tortonian 7 Ma ago (Weijermars *et al.* 1985), and gives some indication of the age of the present morphology in the Betic-Rif orogen.

The collision between the African and European plates has previously been interpreted as the cause of the formation of the former Alboran topographic high (Platt *et al.* 1983, Platt & Behrmann 1986). However, this seems unlikely since the subsequent subsidence of the Alboran Basin needs crustal thinning by either stretching or doming above a mantle diapir with excessive surface denudation (e.g. nappe translations, Fig. 2b). It cannot be explained by the progressive crustal and lithospheric thickening that would occur between two colliding continents.

MAJOR LITHOLOGICAL AND TECTONIC UNITS OF THE EASTERN BETIC ZONE

The Internal or Betic Zone of the Betic Cordilleras comprises predominantly east–west trending mountain ranges and intermontane depressions. Figure 3 is a compilation map of the geology of the eastern part of the Betic Zone. This map shows the spatial distribution of the metamorphic basement ranges (comprising Late Oligocene nappes), intermontane Neogene basins, volcanics and major faults. For comparison, a satellite image of the same area is shown in Fig. 4.

The nappes in the basement are classically grouped into three major tectonic complexes, which regionally

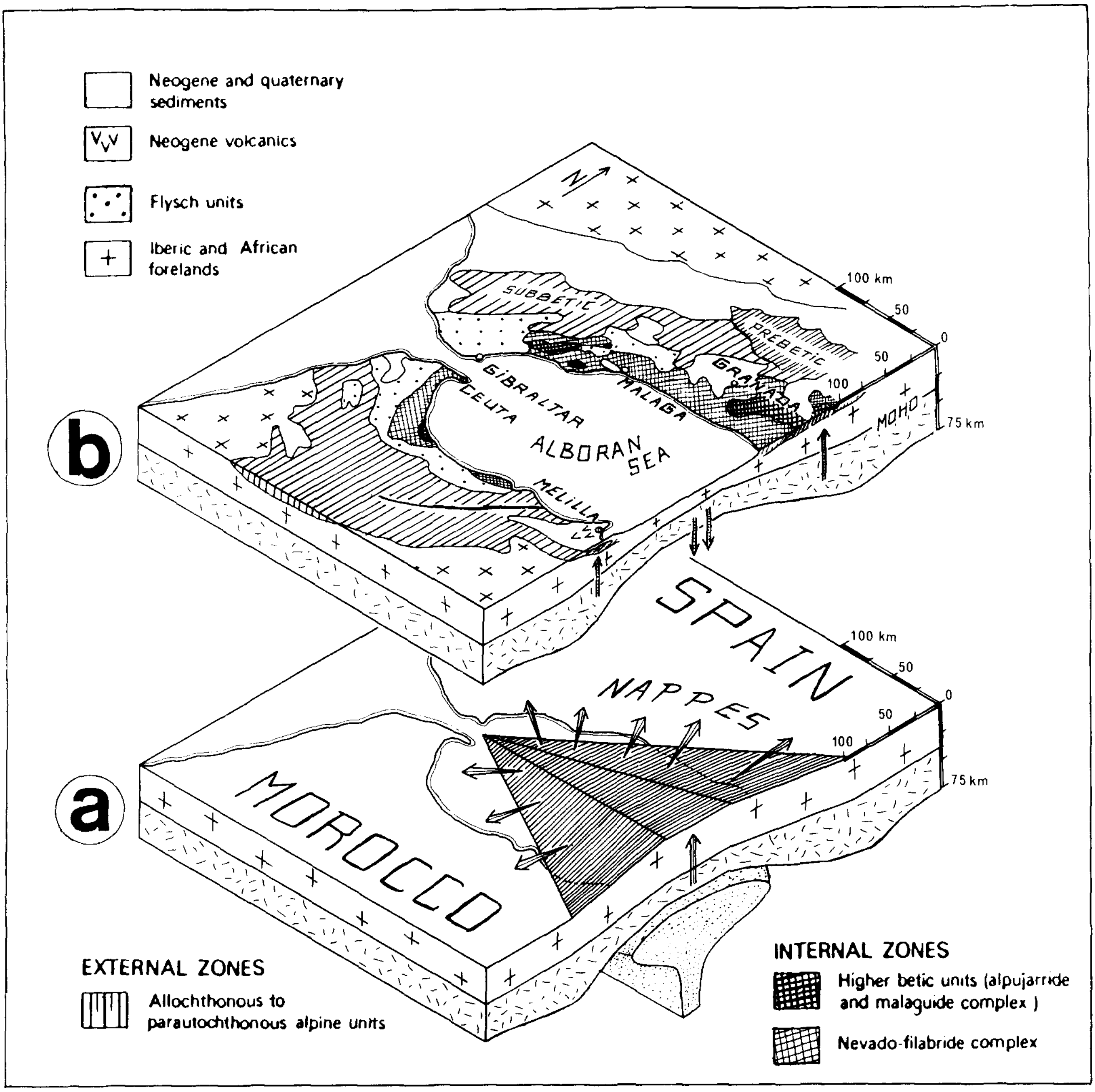

Fig. 2. Successive stages of the Neogene evolution of the Alboran Basin and the Betic-Rif orogen. (a) Nappe-shedding was caused by lithospheric bulging above a mantle diapir emplaced about 20–25 Ma ago. (b) Subsidence of the Alboran Basin followed upon the tectonic unroofing by nappe-shedding after cessation of the diapiric mantle rise and onset of lithospheric cooling about 15–20 Ma ago. Uplift of the Betic-Rif Mountains occurred by isostatic recovery of lithospheric downwarps peripheral to the Alboran Diapir according to a mechanism discussed in detail by Neugebauer (1983, fig. 3).

overlie each other. These are in ascending order: (1) Nevado-Filabride; (2) Alpujarride; and (3) Malaguide complexes (Egeler & Simon 1969a,b, Torres Roldán 1979). The first two nappe complexes are polyphase deformed and consist of mainly metamorphic rocks. The third, mainly non-metamorphic, Malaguide complex occurs only in klippen (too small, i.e. 1 km base length, to be indicated individually) within the area outlined in Fig. 3.

Detailed tectonic analysis in the metamorphic basement of the Sierra Alhamilla has revealed that the morphology of the range is largely controlled by a Neogene anticlinorium (Platt *et al.* 1983, cf. Weijermars 1985c). More specifically, stratigraphical studies in marine sediments along the margins of, and in, the Neogene basins adjacent to the Sierra Alhamilla suggest that the range was principally formed around the Tortonian–Messinian time boundary approximately 7 Ma ago (Weijermars *et al.* 1985). The Alhamilla anticlinorium is asymmetrical with a steep to overturned northern limb which is partly thrust onto the sediments in the Sorbas Basin along the Northern Boundary Fault (Fig. 3). Geological studies in the Sierras de Gador (Jacquin 1970), de Cabrera (Kaper 1981), de los Filabres (Vissers 1981) and de las Estancias (Akkerman *et al.* 1980) have revealed that the general east–west trend of these ranges (Fig. 3) also coincides with the axes of major anticlinoria.

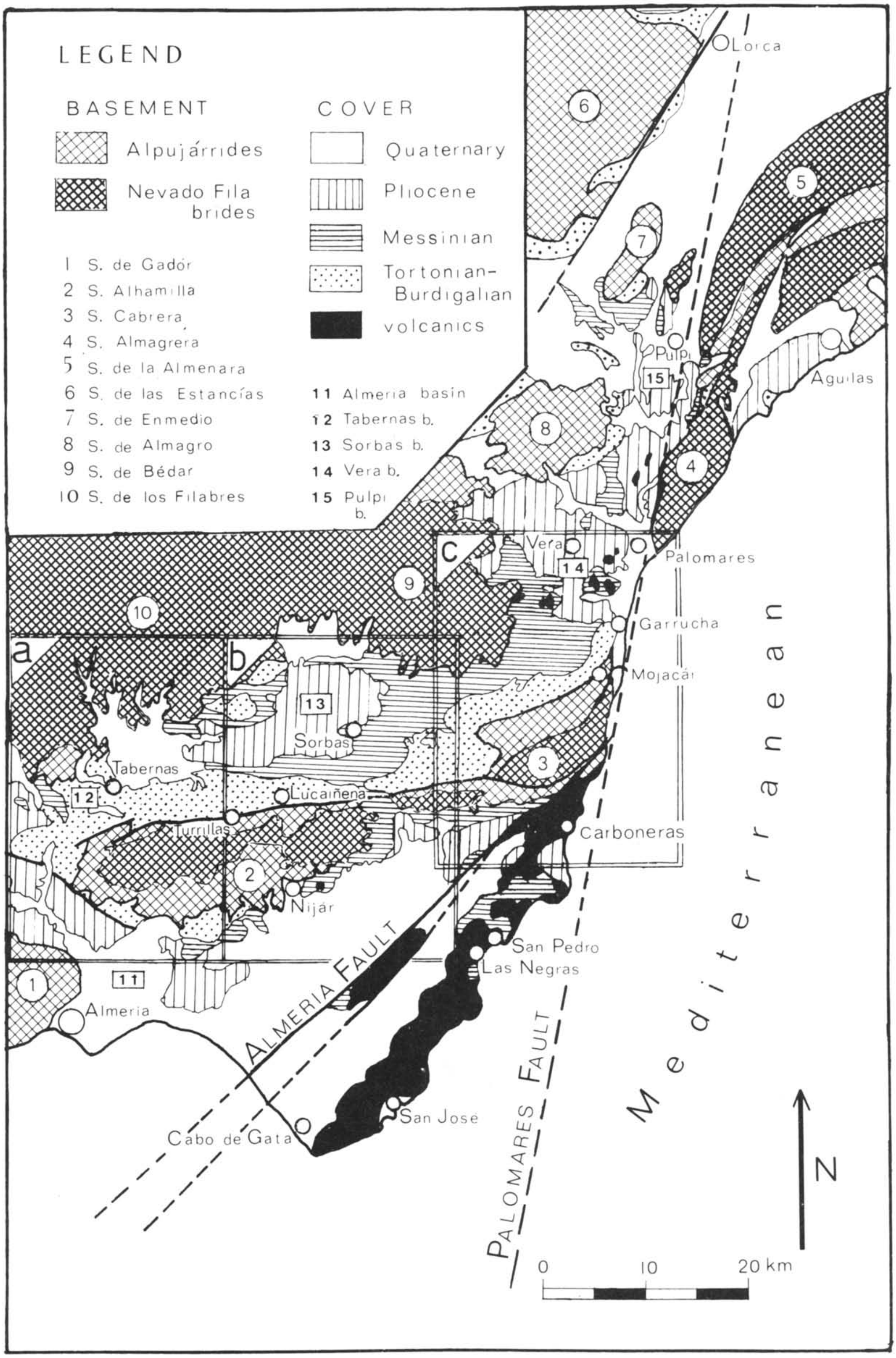

Fig. 3. Geological map of the eastern Betic Zone of the Betic Cordilleras. The major ranges (sierras) and basins are indicated by numbers given in the legend. The outlines of two detailed maps published in Weijermars *et al.* (1985) are labelled a and b. Map c is published in Fig. 6 of this paper. The geological overview of the Neogene basins of southern Spain is compiled here for the first time on the basis of detailed maps published previously (Rondeel 1965, Völk 1967, Veeken 1983, Westra 1969, Weijermars *et al.* 1985), completed with data from student surveys supervised by Dirk Beets (Geological Survey of the Netherlands) and Tom Roep (University of Amsterdam) during the past two decades.

Fig. 4. Multispectral Scanner (MSS) scene of the area outlined in Fig. 3 made by the satellite Landsat 3 on 11th March, 1979, from 920 km height. Shown here are the band-7 data (near-infrared 0.8–1.1 μm wavelength). The scale of resolution is 79 m. The major structural features mapped independently on the ground and compiled in Fig. 3 are visible.

It has been customary to subdivide the Neogene cover into Older Neogene (Burdigalian and Serravallian) and Younger Neogene (Tortonian–Pliocene) according to Völk & Rondeel (1964). The major argument for this subdivision was the sudden change from Alpujarride to Nevado-Filabride detritus. This subdivision cannot be indicated on Fig. 3, because Older Neogene sediments occur mostly as small isolated conglomerate outcrops along the basement margins (see Fig. 6). Instead the Neogene cover in Fig. 3 has been subdivided into: (1) *Burdigalian–Tortonian*: conglomerates and turbiditic sandstones (Völk & Rondeel 1964, Völk 1967); (2) *Messinian*: marine marls (Veeken 1963), barrier reefs (Dabrio *et al.* 1981), gypsum (Dronkert 1976, Pagnier 1976), coastal barrier sequence (Roep *et al.* 1978) and a coastal plain sequence (Geerlings *et al.* 1980); (3) *Pliocene*: subaqueous fan conglomerates (Postma 1984a,b); and (4) *Quaternary*: barranco conglomerates.

Large exposures of calc-alkaline volcanics occur in a magmatic arc-like setting between Cabo de Gata and Carboneras (Fig. 5), which is termed the Cabo de Gata Volcanic Chain (Lodder 1966, Pineda Velasco 1984). The volcanics vary in composition from andesitic to rhyolitic, and K–Ar whole-rock age dating suggests a range in ages from 15 to 8 Ma covering Serravallian–Tortonian times (Bellon 1976, Bellon & Brousse 1977, Bellon *et al.* 1983). Rhyolites and lamproites in the Vera Basin north of the Cabo de Gata Volcanic Chain (Fig. 5) give K–Ar ages between 7.6 and 8.6 Ma (Nobel *et al.* 1981). Further to the north, calc-alkaline volcanics form an interrupted chain between Vera and Cartagena (Fig. 5), which yield K–Ar whole-rock ages between 13 and 6 Ma (Girod & Girod 1977). The Cabo de Gata Volcanic Chain probably continues along strike in a south-westerly direction as a submarine volcanic ridge on the floor of the Alboran Sea (Le Pichon *et al.* 1972). Noteworthy, the volcanic Island of Alboran also has an andesitic composition (Hernandez Pacheco & Ibarolla 1970).

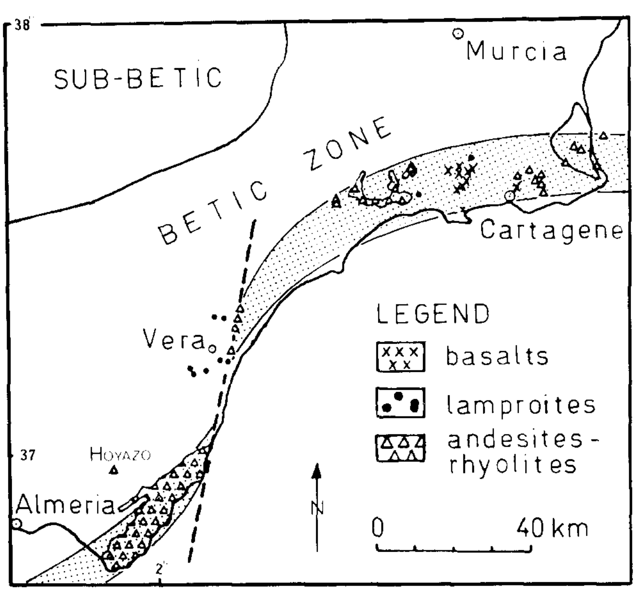

Fig. 5. Neogene volcanics in the Internal Zone of the Betic Cordilleras are predominantly rhyolites–dacites (calc-alkaline volcanics), but basalts and lamproites occur also. The calc-alkaline volcanics may have formed a more or less continuous island arc (shaded) before disruption by the Palomares Fault. The displacement by the Palomares Fault is about 30 km. (Distribution of volcanics after Nobel *et al.* 1981 and Araña & Vegas 1974.)

PALOMARES FAULT AND PALOMARES SHEAR ZONE

The Sierras de las Estancias, los Filabres and Alhamilla-Cabrera are all terminated towards the east by an approximately north–south-striking lineament indicated as the Palomares Fault on Fig. 3. The Palomares Fault was named so by Bousquet *et al.* (1975), but was referred to as the Aguilon wrench-fault by Veeken (1983). The existence of this lineament was first suggested by Völk (1967), who left it nameless.

The gradual change in the strike of the Sierra de Cabrera approaching the Palomares Fault suggests that the walls of this fault are ductilely deformed for a distance of up to 20 km from the Palomares Fault (Fig. 3). Although systematic mapping of the basement inliers east of the Palomares Fault has only begun recently, it is obvious from the regional map pattern that the strikes of the Sierras de Almagrera and de la Almenara are also strongly deflected into the direction of the Palomares Fault (Fig. 3).

The ductilely deformed walls and the brittle Palomares Fault *sensu stricto* are together referred to here as the Palomares Shear Zone. The Palomares Shear Zone is 44 km wide and can be classified as brittle–ductile according to the terminology of Ramsay (1980). The Palomares Fault forms the median surface of the Palomares Shear Zone and is interpreted here as being active while its walls distorted in a ductile fashion.

The term 'ductile' is used here only to distinguish the penetrative non-localised strain in the walls of the Palomares Shear Zone from the localised strain in the brittle Palomares Fault proper. It does not have a mechanistic connotation and agrees with the nomenclature proposed by Rutter (1986). A systematic microstructural study of the rock fabric in the field has not been undertaken, but the mechanisms involved in the formation of the surface pattern of the Palomares Shear Zone are probably pressure solution and cataclastic flow. These mechanisms are the most likely since the rocks that define the modern surface pattern have been at or near the surface for at least 7 Ma (Weijermars *et al.* 1985) and a major part of the shear motion is younger (see later). Shear by crystal plasticity may have occurred at deeper crustal levels and this effective deformation mechanism may have controlled the formation of the surface pattern of the Palomares Shear Zone (Fig. 3).

The sinistral strike–slip sense of the Palomares Shear Zone is obvious from the regional map pattern in Fig. 3. Detailed field observations also support the sinistral sense of shear. Fold axes in the Tortonian Chozas Formation gradually rotate over 20° from E–W in the Sorbas Basin to N70°E in the Vera basin (Rondeel 1965). The particular nature of the shear can be inferred from the

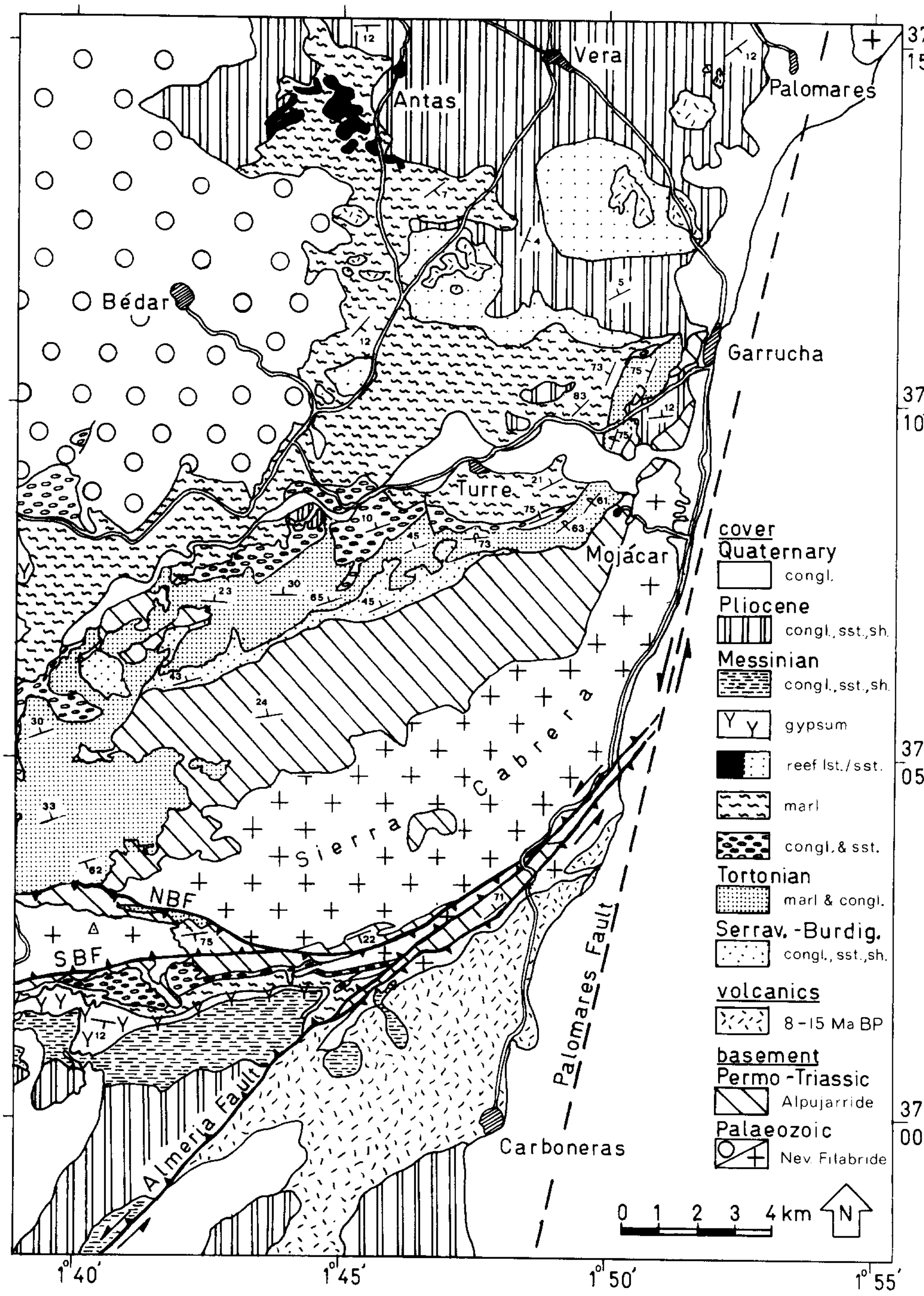

Fig. 6. Geological map of the Sierra Cabrera and Vera Basin shown by outline c in Fig. 3. The Sierra Cabrera's structural trend changes from E–W in the west to NNE–SSW near the Palomares Fault at its eastern termination. The strikes of Older Neogene (Burdigalian–Serravallian), Tortonian and Messinian beds along the southern margin of the Vera Basin show a similar deflection. Gently dipping Lower Pliocene deposits unconformably overlying the steep to overturned older strata (e.g. 1 km SW of Garrucha) suggest that major deflection occurred early in the Lower Pliocene. The Northern Boundary Fault (NBF) and Southern Boundary Fault (SBF) are both Late Tortonian Faults genetically associated with the formation of the anticlinorium in the Alhamilla-Cabrera basement range (cf. Platt *et al.* 1983, Weijermars *et al.* 1985). The lithological map annotation used is the same as that of the detailed maps of the adjoining area in the west published by Weijermars *et al.* (1985). (Compiled on the basis of Rondeel 1965, Völk 1967, and Westra 1969.)

deflection of Tortonian and Messinian strata along the northern boundary of the Sierra Cabrera. These gradually change in both strike and dip towards that of the subvertical Palomares Fault on approaching the fault (Fig. 6). This change in both the strike and dip can be best explained by (either crystalloplastic or cataclastic) necking as clarified by the stratum contour model of Fig. 7.

An alternative interpretation would be that the Palomares Shear Zone has only caused the change in strike (without any necking) and that the gradual change in the dip of the sedimentary beds is due to tilting by differential uplift of the Sierra Cabrera prior to shearing. However, this seems less likely since major differential uplift would then have occurred after the deposition of the now tilted Messinian marls. This is contradicted by the

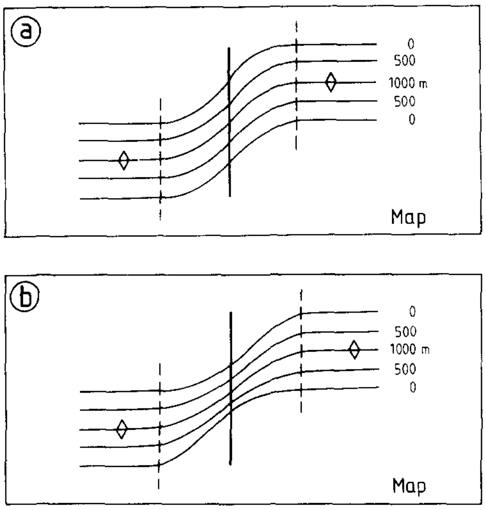

Fig. 7. The effect of shearing upon the attitude of the limbs of an antiform indicated by the stratum contours. (a) The dip of the limbs remains constant and only their original strike is changed by a shear zone without any necking. (b) Both the dip and strike gradually change across a shear zone involving necking.

major episode of differential uplift due to folding near the end of the Tortonian 7 Ma ago (i.e. pre-Messinian) suggested by Weijermars *et al.* (1985).

There is no evidence for any significant vertical shear motion of the Palomares Fault. Horizontal slickensides have been reported from minor strike–slip faults parallel to the trace of the Palomares Fault near Garrucha (Bousquet 1979) and seismic reflection profiles suggest that the crust is equally thick at either side of the Palomares Fault (Banda & Ansorge 1980, cf. Fig. 8).

AMOUNT OF SHEAR ON THE PALOMARES FAULT

Quantification of the horizontal shear involved in the Palomares Shear Zone requires markers which can be correlated across the shear zone. There are two possible candidates: (1) the 8–15 Ma old calc-alkaline volcanic chain between Vera and Cartagena, which initially may have formed a continuous open arc with the Cabo de

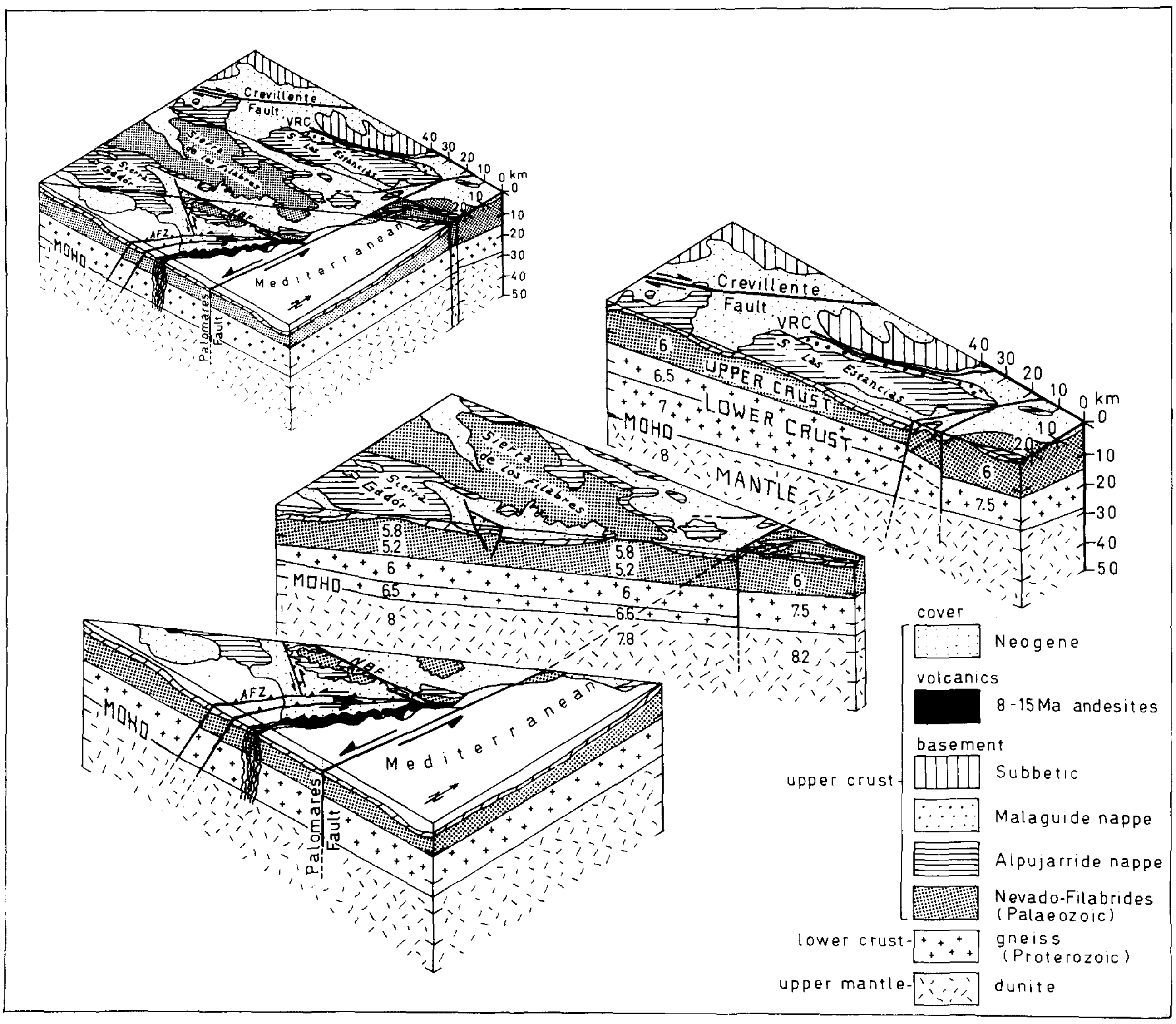

Fig. 8. Isometric block diagram of the crust and part of the upper mantle beneath the eastern Betic Zone. The Palomares Fault transects the entire crust as it juxtaposes two crustal segments with different seismic structures. The seismic velocities indicated are in km s^{-1} and have been inferred from Banda & Ansorge (1980). The NW dip of the Almería Fault Zone (AFZ) is assumed on the basis of the surface observations of Westra (1969). Hermes' (1978, 1984) Velez Rubio Corridor (VRC), a major dextral strike–slip fault, is also indicated.

Gata Volcanic Chain before it was dislocated by the Palomares Shear Zone (Fig. 5); (2) the fold axes of the 7 Ma old basin and ranges on Fig. 3 (dated by Weijermars *et al.* 1985), which probably all had uniform E–W trends before displacement by the Palomares Shear Zone (cf. Bousquet 1975). Both these markers will be discussed here.

It has been suggested that the Cabo de Gata Volcanic Chain (Fig. 3) continues for at least 200 km along strike in a south-westerly direction as a submarine volcanic ridge (Le Pichon *et al.* 1972) on which the calc-alkaline volcanic Island of Alboran is located (Hernandez Pacheco & Ibarolla 1970). It seems therefore reasonable to suggest that this volcanic ridge also continued with a NE–E trend before it was disrupted by the Palomares Fault. It is necessary to emphasize this because the calc-alkaline volcanics of Vera-Cartagena and those of Cabo de Gata have occasionally been interpreted as two distinct volcanic provinces (Araña & Vegas 1974), presumably because the Palomares Fault was not yet recognised.

The hypothesis that all the basins and ranges on Fig. 3 had east–west strikes (7 Ma ago) before displacement by the Palomares Shear Zone would imply that the Alhamilla-Cabrera range is the westward continuation of the Sierra Almagrera and that the Sierra de la Almenara is the displaced continuation of the Sierra de los Filabres (cf. Fig. 3). This view is supported by preliminary surveys, which have revealed that a sedimentary basin is imbricated in between the Sierras Almagrera and de la Almenara (Montenat *et al.* 1978). This imbricated basin could be interpreted as the eastward continuation of the Sorbas and Vera Basins prior to the displacement by the Palomares Shear Zone.

Additional evidence for the gradual deflection and final disruption of an originally E–W striking Alhamilla-Cabrera-Almagrera range is provided by palaeogeographical observations. Völk (1966) suggested that the Vera Basin was a nearly closed marine bay during the Upper Pliocene on the basis of conglomerates in the Upper Pliocene Espiritu Santo Formation which have been deposited in a fluvio-marine environment. The terrigenous detritus and westward transport axes suggest that the Espiritu Santo conglomerate was supplied by a land barrier in the east (i.e. the Sierra Almagrera) which separated the Vera Basin from the Mediterranean during the Upper Pliocene (Völk 1966). This suggests that the modern connection between the Mediterranean and the Vera Basin (Fig. 3) was first established in the Quaternary, after complete separation of the Sierra Almagrera from the Alhamilla-Cabrera range.

The amount of shear implied by the displaced volcanic arc (Fig. 5) is not in agreement with that suggested by the displaced basement inliers (Fig. 3). The 7 Ma old basement pattern of Fig. 3 suggests a displacement of approximately 14 km on the Palomares Fault (see also the discussion on the strain profile of Fig. 9), whereas some 30 km displacement is implied by offset of the 8–15 Ma old volcanic chain (Fig. 5). The discrepancy of 16 km between the two estimates suggests significant displacement of the volcanic chain prior to the formation of the 7 Ma old basin and range structure in the basement. Part of the discrepancy could be due to the higher competence of the volcanics as compared to that of the basement rocks.

The adoption of the two markers discussed above implies that the basins and ranges of the Betic Zone probably were formed whilst the Palomares Fault was already in existence. This could be used to suggest that the basins and ranges on either side of the Palomares Fault may be caused by the shearing itself. However, this seems mechanically unlikely since the axes of the Neogene basin and range structures extend for approximately 300 km throughout the Betic Zone with a trend which is consistently E–W outside the 44 km wide rock volume affected by the Palomares Shear Zone.

It is mechanically plausible that the shallow basin and range structure of the Betic Cordilleras formed during a relatively short time span near the end of the Tortonian about 7 Ma ago. The basins and ranges are due to open folds with an average amplitude of about 1 km and wavelength of 16 km (cf. Weijermars *et al.* 1985). The longitudinal strain involved in the folding can be estimated to be about 0.3 if a buckle mechanism is assumed (cf. Turcotte & Schubert 1982, p. 115). Such a strain can be established in 1 Ma if a typical tectonic strain rate of $10^{-14}\ s^{-1}$ is adopted (cf. Pfiffner & Ramsay 1982).

TIME FRAME AND UNSTEADINESS OF THE PALOMARES SHEAR MOTION

The 30 km displacement of the 8–15 Ma old volcanic chain and the 14 km displacement of the 7 Ma old basin and range structure suggest that the Palomares Fault has been active since at least 8 Ma ago. The ductile deformation of its walls may have occurred coevally with the formation of the axial Palomares Fault, but may also have started during an advanced stage of shearing along the Palomares Fault (but not later than 5 Ma ago, see below). The off-set of Quaternary sediments and, near Garrucha, an Early Tyrrhenian marine terrace, by minor strike–slip faults parallel to the Palomares Fault suggests that the main fault is still active (Bousquet 1979).

There are several indications that the motion along the Palomares Fault and the formation of the Palomares Shear Zone occurred by unsteady activity. The most recent evidence is provided by a major earthquake, which destroyed the city of Vera in 1518 and is thought to have been generated by the Palomares Fault (Bousquet 1979). Another major episode of activity in the Palomares Shear Zone seems to have occurred after the Messinian early in the Lower Pliocene between 4 and 5 Ma ago. This can be inferred from stratigraphical observation in two areas.

(1) Along the northern margin of the Sierra Cabrera, gently dipping Lower Pliocene sediments of the Cuevas Formation unconformably overlie steep to overturned Burdigalian to Messinian deposits (Fig. 6). The unconformity gradually changes into a conformity westwards

towards the boundaries of the Palomares Shear Zone (Fig. 3, and Pliocene outcrops too small to be indicated on Fig. 6). This suggests that *major* displacement occurred early in the Lower Pliocene before deposition of the Cuevas Formation (cf. Fig. 6). The tilted sediments of the Older Neogene and Tortonian Chozas and Messinian Turre Formations are relatively undisturbed internally when compared to the overlying Lower Pliocene Cuevas Formation, which contains intraformational unconformities (Völk 1967).

(2) The basin imbricated between the Sierra Almagrera and de la Almenara (Fig. 3) contains intensively fractured and steeply tilted Langhian and Serravallian sediments, which are also unconformably overlain by relatively undisturbed Lower Pliocene deposits (Montenat *et al.* 1978). This suggests that the major imbrication event may have occurred contemporaneously with major movements on the Palomares Fault between 4 and 5 Ma ago early in the Lower Pliocene. A subsequent discovery of pseudotachylites along the trace of the Palomares Fault would confirm its palaeoseismicity (cf. Sibson 1980).

The about 14 km displacement along the Palomares Fault (Fig. 9b) in the past 7 Ma implies a mean displacement rate of 2 mm a^{-1}. This is rather slow compared to the extremely fast displacement rate of 5.5 cm a^{-1} presently observed for the San Andreas Fault (Turcotte & Schubert 1982, p. 101). However, it is likely that the mean shear rate of the Palomares Fault has been higher during its periods of major activity. This may have been the case, for example, in the 15th century when the Vera earthquake occurred and in the Lower Pliocene (4–5 Ma ago) when earthquakes generated by the Palomares Fault caused intraformational unconformities in the coeval Cuevas Formation (Völk 1967; cf. Seilacher 1984) of the area outlined in Fig. 6. I assume that the modern shear rate of 5.5 cm a^{-1} for the San Andreas Fault gives a representative value for the mean shear rate of strike-slip shears in a period of major activity. This suggests that deviations of about one order of magnitude from the mean displacement rate estimated for the Palomares Fault may have occurred during the periods of its major seismic activity.

LATERAL TERMINATORS OF THE PALOMARES FAULT: THE ALHAMA DE MURCIA FAULT AND THE ALMERIA FAULT ZONE

The Palomares Fault has previously been interpreted as a fault which either originates from or terminates against the NNE–SSW striking Alhama de Murcia Fault (Bousquet & Montenat 1974, Bousquet & Philip 1976a), which truncates the Sierra de las Estancias south of Lorca (Figs. 3 and 4). Gravimetric and electrical lineaments have been used to infer that the Alhama de Murcia Fault extends towards the NE up to Alicante (Gauyau *et al.* 1977), where it joins the Crevillente Fault (Fig. 1).

Along the southward extension of the Palomares Fault, two major 200–300 m wide NE–SW trending imbricate reverse faults dipping about 70° NW have been mapped at the southern flank of the Sierra Cabrera (Fig. 6) (Westra 1969). Both fault zones include slices of Serravallian marls, Neogene volcanics and rocks from the Alpujarride and Malaguide nappe complexes (Kaper 1981). The rock volume affected by both faults has been termed the La Serrata Fault (unreferenced in Baena *et al.* 1977), the Carboneras Fault Zone (Bousquet *et al.* 1975, Bousquet & Philip 1976a,b) or the Almería Fault Zone (Baena *et al.* 1977, Greene *et al.* 1977, Postma 1984b). The term Almería Fault Zone is adopted here.

Previous maps of the Almería Fault Zone are highly suggestive towards an interpretation that this fault is the southeastward continuation of the Palomares Fault (Bousquet *et al.* 1975, Bousquet & Philip 1976a,b). This would imply an abrupt change in the strike of a major wrench fault which is mechanically unlikely. I interpret the Almería Fault Zone as a splay or second-order fault of the Palomares Fault. It presumably formed in a late stage of the formation of the Palomares Shear Zone since its trend is not deflected into that of the Palomares Fault such as observed in the outcrop pattern of the basement ranges (see Figs. 3, 4 and 6).

The straight boundaries of isolated volcanic outcrops in the Almería Fault Zone (Fig. 3) are taken to indicate that the volcanics predate the faulting. These volcanics have ages similar to those determined for the Cabo de Gata volcanics (i.e. 9–15 Ma, Bellon *et al.* 1983), which suggests that the Almería Fault Zone is younger than 9 Ma. Steeply dipping Messinian reefs unconformably overlain by Pliocene calcarenites within the Almería Fault Zone (Van de Poel pers. comm. 1980) suggest the occurrence of major fault movements somewhere between Messinian and Pliocene times. As the morphology of the submarine slope near Cabo de Gata appears to suggest hundreds of metres sinistral strike-slip displacement, the Almería Fault Zone may extend into the Gulf of Almería (Fig. 3) (Greene *et al.* 1977). Such morphology also indicates recent activity of the Almería Fault Zone.

It is tempting to suggest that both the Palomares and Almería Faults transect the floor of the Alboran Sea to join the Nekor and Jedha Faults in North Africa, respectively (Fig. 1). However, confirmation of this requires detailed mapping of the Alboran Sea floor.

DEPTH OF THE PALOMARES FAULT

One of the possible modes of shear zone termination is by dispersal of the total shear strain involved in the displacement over a wider rock volume (cf. Simpson 1983). Termination of megashears by shear zone widening is favoured at deep crustal levels because other shear fault terminations would involved brittle solutions. Two seismic reflection profiles across the Palomares Fault indicate that the crustal segments on either side of the fault have entirely different seismic structures (Banda & Ansorge 1980) suggesting that the fault plane transects

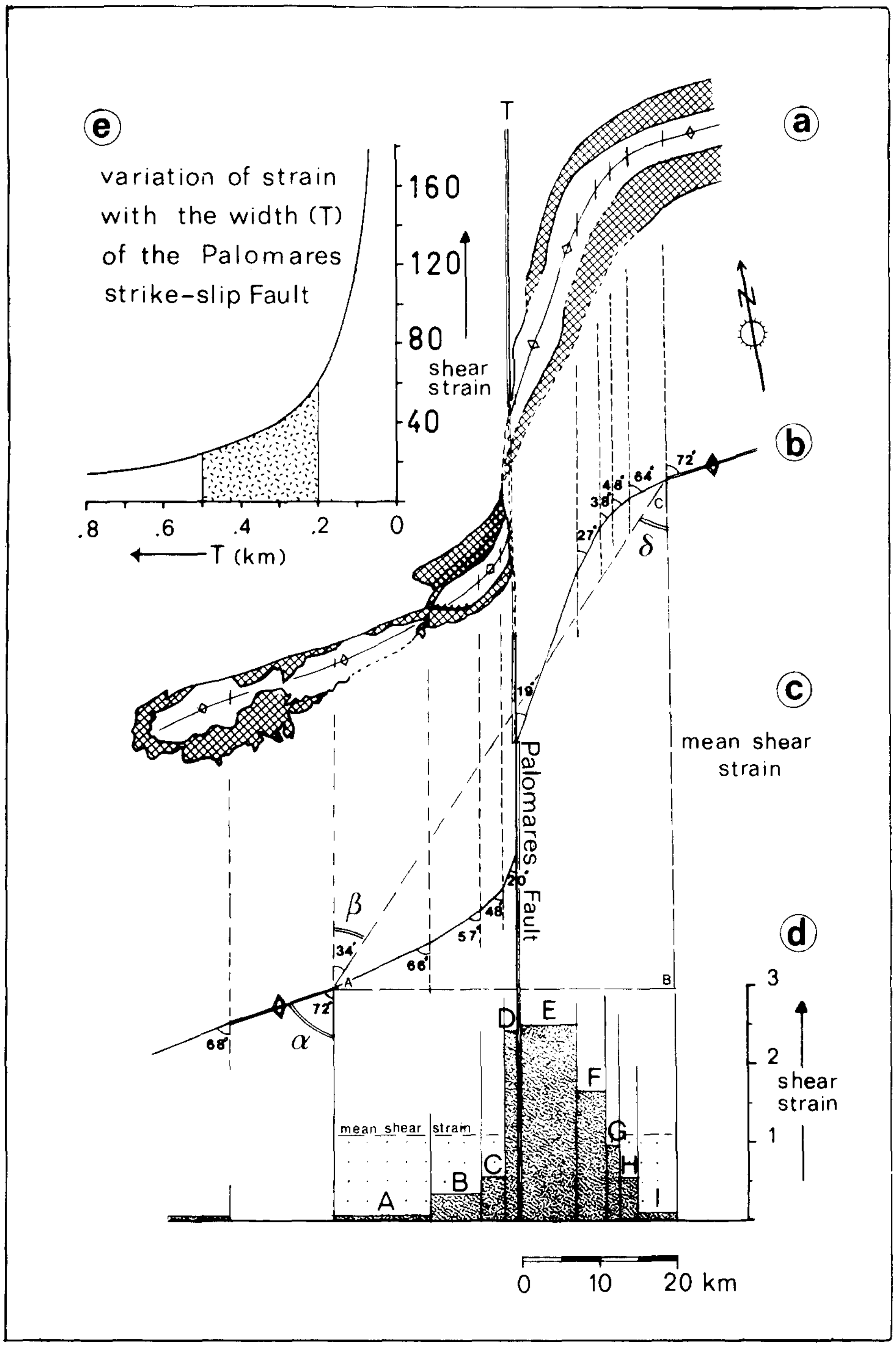

Fig. 9. Working method to quantify the shear strain across and along the Palomares brittle–ductile Shear Zone. (a) The outcrop pattern of the deflected and disrupted Alhamilla-Cabrera-Almenara chain is redrawn from Fig. 3 and the anticlinorium fold axis acts as strain marker line. (b) Arbitrary subdivision of the marker line in segments of straight strike to enable computation of the shear strain of each segment from the angular deflection of the strain marker by applying equation (1). (c) Construction of the mean shear strain across the entire width of the Palomares Shear Zone: cot 34° − cot 72° = 1.16. (d) Strain–distance histogram across the Palomares Shear Zone. The western wall (segments A–D) has shear strains:

$$\begin{aligned} A &= \cot 66° - \cot 72° = 0.12 \\ B &= \cot 57° - \cot 72° = 0.33 \\ C &= \cot 48° - \cot 72° = 0.58 \\ D &= \cot 20° - \cot 72° = 2.42. \end{aligned}$$

The mean shear strain of the 23.5 km thick western wall is:
[(0.12·12.8 km) + (0.33·6.4 km) + (0.58·2.9 km) + (2.42·1.4 km)]/(23.5 km) = 0.37.
The eastern wall (segments E–I) has shear strains:

$$\begin{aligned} E &= \cot 19° - \cot 72° = 2.58 \\ F &= \cot 27° - \cot 72° = 1.64 \\ G &= \cot 38° - \cot 72° = 0.95 \\ H &= \cot 48° - \cot 72° = 0.57 \\ I &= \cot 64° - \cot 72° = 0.16. \end{aligned}$$

The mean shear strain of the 20.5 km thick eastern wall is:
[(2.58·7.2 km) + (1.64·3.6 km) + (0.95·1.8 km) + (0.57·2.5 km) + (0.16·5.4 km)]/(20.5 km) = 1.39.
(e) Strain–width diagram which shows the shear strain variation with the width (T) of the Palomares Fault on the basis of equation (5). The shaded area indicates how the shear strain varies between 70 and 28 if a variation of T between 0.2 and 0.5 km is assumed.

the entire 23–30 km thick crust in SE Spain. Banda & Ansorge (1980) also suggest that the seismic data might indicate a widening of the Palomares Fault near the base of the crust. The surface geology and crustal structure revealed by the two seismic reflection profiles are integrated in an isometric block diagram of the upper lithosphere in the Eastern Betic Zone (Fig. 8). The seismic profiles do not resolve the structured layering of the upper mantle (or lower lithosphere, see Banda & Ansorge 1980, fig. 13). This leaves open the possibility that the crust is detached from the lower lithosphere by a horizontal shear zone to accommodate the strike–slip displacement along the vertical Palomares Shear Zone. Such a mechanism has been proposed for the downward termination of major shear zones in the Limpopo belt (Coward 1980).

Banda & Ansorge (1980) contended that their data indicate the upper crust to comprise mainly Nevado-Filabride rocks, a view which is adopted here. Migmatitic gneiss occurring as xenoliths in andesitic volcanics at El Hoyazo (Zeck 1970) 3 km to the east of Nijar (Fig. 3, cf. Fig. 5) may be representative of the composition of the lower crust as indicated in Fig. 8. Tentative Rb–Sr ages of 800 Ma have been obtained from these gneiss xenoliths (Zeck 1970) implying that Proterozoic basement probably occurs beneath the Palaeozoic rocks of the Nevado-Filabride complex.

SHEAR STRAIN PROFILE ACROSS THE PALOMARES SHEAR ZONE

A standard technique to quantify the amount of angular shear strain γ across ductile shear zones uses the angular deflection of the trace of a passive strain marker line (Ramsay & Graham 1970). The acute angle α between such a strain marker line and the shear zone before the shearing (as can be determined outside the sheared rock volume) is reduced to angle β after a shear strain γ with a magnitude (Ramsay & Graham 1970):

$$\gamma = \cot\beta - \cot\alpha. \tag{1}$$

If the strain marker line is gradually deflected into the shear direction, then the angle β varies with position x along an axis normal to the shear direction. The total shear (s) across the shear zone is then represented by the integral (cf. Ramsay & Graham 1970).

$$s = \int_{x_1}^{x_2} \gamma \, dx. \tag{2}$$

The solution of this integral can be represented in so-called strain–distance graphs. Clear practical examples have been discussed by Ramsay & Huber (1983), Simpson (1983) and Weijermars & Rondeel (1984).

Construction of strain–distance graphs across *brittle–ductile* shears like the Palomares Shear Fault is more complex than that for ductile shears because potential strain marker lines are characteristically disrupted in the central part of any brittle–ductile shear zone. In the case of the Palomares Shear Zone this disruption is due to the Palomares Fault (Fig. 3).

The shear strain analysis discussed here concentrates on that part of the strain history of the Palomares Shear Zone which can be inferred from the deflected fold axes of the 7 Ma old basement ranges. This approach is chosen for two reasons. Firstly, it leads to an estimate of the mean shear strain (since 7 Ma ago) for the bulk of the crustal rocks involved in the shear. This seems more representative than that indicated by the strained volcanics which may have different mechanical properties and occupy only a relatively minor part of the total rock volume affected by the shear. Secondly, the age of the basin and range structure is better constrained than that of the volcanics and hence allows better estimates for the mean shear strain rates (since 7 Ma ago) than the volcanics with a broad range of ages.

A shear strain profile of the deformed walls on either side of the Palomares Fault is constructed by using the angular deflection of the axis of the Alhamilla-Cabrera-Almagrera range as a passive strain marker line (Fig. 9a). This axis is subdivided into arbitrary segments δx of consistent trend (Fig. 9b) so that a strain–distance histogram can be constructed from these segments (Fig. 9d).

The shear strain within the Palomares Fault itself cannot be constructed by the method outlined above, because both its width and the angle with the strain marker are unknown. However, another method to resolve the strain magnitude across the Palomares Fault is presented.

The mean shear strain of 1.16 across the entire 44 km width of the Palomares Shear Zone can be constructed on a map by connecting the undeformed segments of the strain marker by a straight line and application of equation (1) (Fig. 9c). The mean shear strain in the deformed walls on either side of the Palomares Fault can be retrieved from the equation:

$$\gamma = \frac{1}{x}\sum_{x_1}^{x_2} \gamma \, \delta x \tag{3}$$

with strain marker segments δx. Equation (3) gives a mean shear strain of 0.37 for the 23.5 km thick western wall and 1.39 for the 20.5 km thick eastern wall of the Palomares Shear Zone.

The mean shear strain of 1.16 across the entire width of the Palomares Shear Zone and the mean shear strains of 0.37 and 1.39 of the deformed walls of the Palomares Fault relate to the shear strain ξ of the Palomares Fault proper by the expression:

$$\begin{aligned}\xi T(\text{km}) &= 1.16 \cdot 44 \text{ km} \\ &\quad - (0.37 \cdot 23.5 \text{ km} + 1.39 \cdot 20.5 \text{ km}) \\ &\cong 14 \text{ km}\end{aligned} \tag{4}$$

where T is the width of the Palomares Fault and ~14 km its total shear since 7 Ma ago. Two assumptions underlying equation (4) are: (1) that there is no volume change involved in the deformation, and (2) that the thickness T of the Palomares Fault is so small compared to the entire width of the Palomares Shear Zone that it has no significant effect upon the estimate of 1.16 for the mean shear strain constructed in Fig. 9(c). A general form of equation (4), and its proof, are in preparation.

The variation in shear strain ξ with width T (in km) for various possible widths of the Palomares Fault can be found from equation (4) by the expression:

$$\xi(T) = 14/T \qquad (5)$$

and has been plotted for a series of arbitrary T-values in Fig. 9(e). The actual width of the Palomares Fault is unknown since it is nowhere fully exposed, but it is tentatively assumed that the major fault plane may be of the order of 0.2–0.5 km wide implying shear strains of between 70 and 28.

SHEAR STRAIN RATE AND VISCOSITY ESTIMATES FOR THE PALOMARES SHEAR ZONE

The shear strains involved in the motion of the Palomares Shear Zone during the past 7 Ma may be used to convert the observed shear strains into shear strain rates. The mean shear strains of 0.37 and 1.39 in the west and east sides of the Palomares Shear Zone, respectively, give respective mean engineering shear strain rates ($\dot{\gamma}$) of (0.37/7) Ma^{-1} or $1.7 \times 10^{-15} s^{-1}$ and (1.39/7) Ma^{-1} or $6.3 \times 10^{-15} s^{-1}$. The mean shear strain of 1.16 across the entire width of the Palomares Shear Zone gives a typical shear strain rate of $5.3 \times 10^{-15} s^{-1}$. The mean shear strain of 28–70 estimated for the Palomares Fault proper suggests relatively rapid shear strain rates varying between 1.3×10^{-13} and $3.2 \times 10^{-13} s^{-1}$.

These engineering strain rates relate to the *tensor* shear strain rate ($\dot{e}$) by the expression (cf. Means 1976, p. 182):

$$\dot{\gamma} = 2\dot{e}. \qquad (6)$$

This implies that the maximum engineering shear strain rate estimated above corresponds to a tensor shear strain rate of $6.5 \times 10^{-12} s^{-1}$ which is extremely fast if compared to the typical range of natural (tensor) shear strain rates of 10^{-13}–$10^{-15} s^{-1}$ compiled by Pfiffner & Ramsay (1982). The other values estimated here lie within this range of common strain rates.

Deviations of about one order of magnitude from the mean shear rate of 2 mm a^{-1} may have occurred during the past 7 Ma of movement on the Palomares Fault, as has been suggested on the basis of the geological arguments discussed above. Variations of say a factor 10 may have occurred in both the shear rates and shear strain rates in the Palomares Fault proper at shallow seismic levels, but may be less for its ductile walls and deeper parts. Assuming that the surface pattern of the Palomares Shear Zone is largely due to crystalloplastic deformation at deeper crustal levels (preferentially involving detachment from the upper mantle) some preliminary estimates of bulk crustal viscosities could be made. Time dependent variations in the shear strain rates will be neglected in what follows. The flow may be either Newtonian or non-Newtonian.

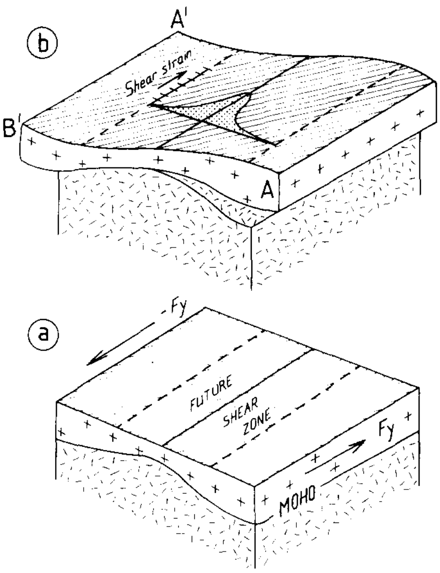

Fig. 10. One possible mechanism of shear zone formation involves an initially thinned crust which is mechanically detached from the underlying upper mantle due to a force F_y acting on the sides of the crustal section outside and parallel to the zone of crustal thinning. (a) The deviatoric stresses in the crust caused by F_y are largest where the crust is thinnest (cf. equation 7). (b) This may lead to the formation of a vertical strike–slip zone above the crest of the bulge in the upper mantle supporting the thinned crust. The typically peaked shear strain profile could thus be formed even in the absence of any flow softening mechanism (i.e. even if the viscosity of crust were to be constant in all directions). Lateral termination of both the horizontal subcrustal and vertical shears may lead to crustal thinning by extensional tectonics at locations A and A′ and crustal thickening by compression at B and B′.

First, one possible mechanism of shear localization in strike–slip shear zones not previously considered needs to be discussed and excluded so that a constant deviatoric stress can be assumed later on. This simple mechanism involves a pre-existing zone of either lithospheric or crustal thinning (or both). It is illustrated in Fig. 10 for a thinned crust, which is assumed to be detached from the underlying mantle (e.g. by a horizontal shear zone, cf. Coward 1980). Two balanced forces F_y and $-F_y$ work in opposite direction on either side of the crustal segment containing the future vertical shear zone (Fig. 10a) and cause a deviatoric stress τ_y which is inversely proportional to the thickness of the crust (d):

$$\tau_y = F_y/d \cdot n_y \qquad (7)$$

with a horizontal unit vector $n_y = (0, 1, 0)$ parallel to the shear direction.

Obviously, τ_y increases rapidly when d decreases and reaches a maximum where the crust is thinnest. Crystalloplastic flow may occur if τ_y is large enough to overcome the particular yield stress and lasts longer than the Maxwell relaxation time. The flow may be either Newtonian or non-Newtonian, and the result will be a ductile shear zone with a typically peaked strain profile as illustrated in Fig. 10(b).

If the mechanism illustrated in Fig. 10 applies to the Palomares Shear Zone no viscosity estimates could be made because it would then be unreasonable to assume that deviatoric stresses are constant throughout the entire crustal section occupied by the shear. However, Banda & Ansorge's (1980) seismic sections suggest that there is no significant crustal thinning involved in the Palomares Shear Zone (Fig. 8).

Assume now that (1) the Palomares crust is mechanically detached from the upper mantle (e.g. a horizontal subcrustal shear zone), (2) the surface strain pattern of the Palomares Shear Zone is approximately congruent with that at depth, and (3) the deviatoric stresses are constant both in space (44 km wide, 30 km deep, 80 km long at least) and time (7 Ma). These admittedly crude assumptions allow the definition of an effective viscosity (η_{eff}) which may only vary in the horizontal x-direction perpendicular to the shear direction:

$$\eta_{eff} = \tau_y/2\dot{e}_y. \quad (8)$$

Similar definitions have been used for the vertically averaged viscosity of the lithosphere in numerical models of the lithospheric thickening in the Tibetan plateau due to the convergence of India with Asia (England & Houseman 1985).

To solve expression (8) I adopt the deviatoric stress of 100 MPa assumed in lithospheric deformations by Turcotte & Schubert (1982) and Bott & Kuznir (1984). The surface pattern of the Palomares Shear Zone suggests that the tensor shear strain rates vary between maxima of $6.5 \times 10^{-12}\,s^{-1}$ in the Palomares Fault and $10^{-17}\,s^{-1}$ at its boundaries. The strains caused by strain rates smaller than $10^{-17}\,s^{-1}$ would all remain invisible on the space (44 km) and time (7 Ma) scales considered here. It could only cause a maximum strain of about 0.6% which corresponds to a strain marker line deflection less than 1°. The maximum strain rate of $6.5 \times 10^{-12}\,s^{-1}$ corresponds to an effective viscosity of (cf. equation 8): (100 MPa)/($1.3 \times 10^{-13}\,s^{-1}$) = 4×10^{20} Pa s. The maximum strain rate of $10^{-17}\,s^{-1}$ at the boundaries and outside the Palomares Shear Zone corresponds to a minimum effective viscosity of 10^{25} Pa s which may be considered rigid for the time scale (7 Ma) and stress levels (100 MPa) considered here. The complete profile of the effective viscosity would have the shape of the strain profile illustrated in Fig. 9(d). Mean effective viscosities of 9×10^{22} Pa s and 3×10^{22} Pa s could be estimated for the west and east walls of the Palomares Fault, respectively. For comparison, the bulk dynamic viscosities of crustal rocks subjected to similar stresses in bending slabs have been estimated at 10^{22} Pa s (Kunze 1980), 2×10^{23} and 4×10^{24} Pa s (Sleep & Snell 1976), 10^{24}–10^{25} Pa s (Beaumont 1978), and 10^{25} Pa s (McNutt & Parker (1978).

KINEMATIC INTERPRETATION OF THE PALOMARES SHEAR ZONE

It seems appropriate to finish this paper by discussing four obvious questions about the nature and origin of the Palomares Shear Zone. (*1*) Why is it located and oriented as it is? (*2*) Why is the viscosity decreasing within the shear zone? (*3*) Why is the shear zone 44 km wide? (*4*) Why is the strain profile (and thus the viscosity profile) asymmetric (cf. Fig. 9d)?

A detailed answer to *Question* (*1*) would require analysis of the stress field and tectonic structure of an area which is beyond the scope of the present paper. It seems likely that the dextral Crevillente Fault is a first order fracture and that the sinistral Alhama de Murcia and Palomares Faults are second and third order fractures, respectively (Fig. 1). Their geometric pattern and sense of shear suggest that the maximum principal compressive stress axis lies somewhere about NNW–SSE.

Question (*2*) can be considered in terms of the mechanisms that may reduce the viscosity (flow softening) in shear zones: geometric, structural, strain, strain rate and thermal softening [see Poirier's (1980) equation (7)]. If the deformation were dominated by diffusion creep (whether Nabarro-Herring or Coble) the constitutive flow law could be written:

$$\dot{e}_y = A\tau_y \quad (9)$$

with the proportionality factor A mainly accounting for the activation energy of vacancy migration and variations in grain size, temperature and confining pressures. The effective viscosity of equation (8) can then be rewritten by inserting τ_y from equation (9):

$$\eta_{eff} = 1/(2A). \quad (10)$$

Note that this viscosity is Newtonian in the sense that it is independent of deviatoric stress variations, but still variable if A is not constant. In strike–slip shear zones subjected to this rheological regime, the viscosity could drop due to either thermal softening or structural softening by grain size reduction. Strain-rate softening cannot occur in diffusion creep and strain softening would require changes in the stress excluded here after rejecting the model of Fig. 10.

Geometric softening could occur when either the slip planes in single crystals or the entire rock fabric rotate into orientations for which the deviatoric shear stress is higher. Slip-plane orientation in crystals of polycrystalline rock seems not very effective (Poirier 1980) but reorientation of the rock fabric and development of new slip planes (e.g. shear band cleavage) may cause effective geometric softening in rocks. Shear band cleavage seems to develop only above differential shear strains of 3 (Weijermars & Rondeel 1984) and is therefore unlikely to have contributed to flow softening in the walls of the Palomares Fault where shear strains are lower than 3 (Fig. 9d). However, it may occur in the Palomares Fault proper and photographs published by Bousquet & Philip (1976, figs. 7–9) suggest that it occurs at least along the trace of the Alhama de Murcia Fault. Noteworthy, this type of geometric softening is not accounted for in the factor A of the constitutive flow law since equation (8) is only valid for isotropic rocks.

Alternatively, structural softening by grain size reduction alone could have caused the minimum drop in the vertically averaged viscosity of at least 10^5 Pa s ($10^{25} \rightarrow 10^{20}$ Pa s) suggested for the Palomares Shear Zone. The proportionality factor A of diffusion creep laws (cf. Poirier 1985) contains the grain size to the second power (Nabarro–Herring creep) or to the third power (Coble creep) so that a minimum viscosity drop of 10^5 Pa s could be brought about by grain size reductions of 300 to 50 times, respectively. This grain size reduction may have caused mylonitisation of the Palomares Fault. It was possibly triggered by a local strain rate increase due to geometric softening when the originally E–W striking main foliation and bedding were deflected into the Palomares Fault. The cause of the initial geometric softening lies in the answer to *Question (1)*.

Shear heating (Brun & Cobbold 1980, Fleitout & Froidevaux 1980) on the Palomares Fault may also have contributed to lower the viscosity of the rock in its walls. This mechanism is particularly attractive since it could potentially solve *Questions (3)* and *(4)*, in a fashion which is only qualitatively investigated here. The distance l of the leading edge of a propagating heat front from a heat source can be estimated from the equation (cf. Turcotte & Schubert 1982, p. 154):

$$l = (\kappa t)^{1/2} \tag{11}$$

with thermal diffusivity κ and time period t since the onset of the temperature increase on the fault plane by friction. Taking half the width of the Palomares Shear Zone for l (=22 km) and an average κ for rocks of 1 mm^2 s^{-1} (cf. Turcotte & Schubert 1982) would imply that the Palomares Fault started producing heat 15 Ma ago if its current 44 km width were determined by thermal softening. It may even have formed later and still have its width controlled by thermal softening if the thermal diffusivity were larger than the 1 mm^2 s^{-1} assumed. However, a formation of the Palomares Fault about 15 Ma ago is still possible within the geological constraints discussed here.

Question (4) can possibly be answered by an eastward dip of the Palomares Fault, so that the viscosity of its east wall would be more affected by shear heating than that of the west wall (Fig. 11). Estimates of the temperature increase required to explain quantitatively the inferred viscosity drop in the walls of the Palomares Fault depends upon the adoption of a particular flow law for a particular rock type (cf. Fleitout & Froidevaux 1980) considered representative for the entire crustal volume of the Palomares Shear Zone and is left beyond discussion.

I consider rocks to strain dominantly by dislocation and not diffusion creep at the deviatoric stresses common in crustal deformation (cf. Weijermars & Schmeling, 1986). The constitutive flow law for a shear flow dominated by one particular mechanism would then be:

$$\dot{e}_y = A\tau_y^n \tag{12}$$

with power n larger than 1 for dislocation creep. Insertion of $\tau_y = (\dot{e}_y/A)^{1/n}$ in equation (8) yields an expression for the effective viscosity which is sensitive to the strain rate $\dot{e}_y$:

$$\eta_{\text{eff}} = \frac{1}{2A^{1/n}}\cdot\dot{e}_y^{(1/n)-1} = 1/(2A^{1/n}.\dot{e}_y^{1-(1/n)}). \tag{13}$$

Viscosity reduction or flow softening by grain size reduction, thermal and geometric softening as discussed for diffusion creep would still occur, but, in addition true strain-rate softening would contribute to the drop of the viscosity across the Palomares Shear Zone. It follows from equation (12) that, if τ_y is constant, as assumed here, any increase of A due to structural and/or thermal softening (geometric softening is not accounted for by A) will also demand an increase of $\dot{e}_y$. This implies that strain-rate softening [due to changes in A and not τ, cf. equation (13)] will then automatically accompany any structural and/or thermal softening (affecting A).

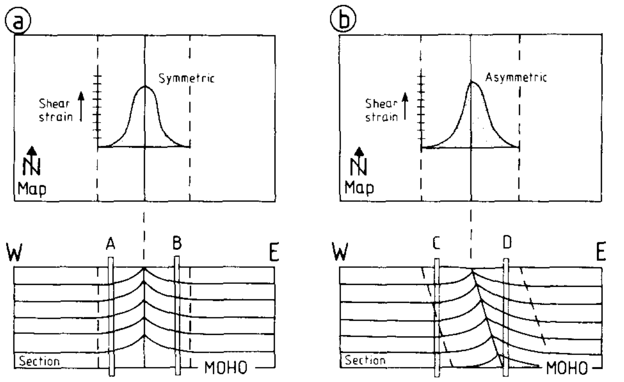

Fig. 11. One possible explanation for the asymmetry of shear strain profiles across (brittle–)ductile shear zones involves shear heating. Arbitrary isotherms are indicated in the lower sections and hypothetic shear strain profiles that could possibly be inferred from deflected surface markers are indicated in the upper maps for each area. (a) Section and map of a vertical strike–slip shear zone in the crust. The shear zone is due to thermal softening by frictional heat from the fault in its core. An orthogonal profile of the isotherms is symmetric about the fault trace. Measurements in boreholes A and B would yield equal vertically averaged temperatures. Accordingly, the thermal softening of the rocks on either side of the fault is similar resulting in a symmetrical strain profile across the shear zone. (b) Section of isotherms and shear strain profile across an eastward dipping strike–slip shear zone. The diffusion length of the frictional heat is equal in either direction perpendicular to the fault plane, but any profile of isotherms is asymmetric. Measurements in borehole D would yield vertically averaged temperatures higher than those of borehole C. The difference in thermal softening of the walls on either side of the fault will result in an asymmetric shear strain profile across the shear zone. Surface heat flow at location D will also be larger than at location C.

The formation of shear zones by non-Newtonian creep therefore will generally occur at higher strain rates than those formed by Newtonian creep if deformed under otherwise equal conditions.

CONCLUSIONS

Detailed research mainly from Spanish, French and Dutch projects has greatly improved understanding of the Betic-Rif orogen. The nappes exposed in the internal zones of the Betic-Rif orogen seem to be emplaced due to bulging of the crust above the Alboran Diapir about 25 to 20 Mg ago. The thinned crust above the Alboran Diapir started to cool about 20 to 15 Ma ago and consequently sank to create the Alboran Basin (Fig. 2). The Betic-Rif Mountains were progressively elevated by isostatic recovery of downwarped lithosphere peripheral to the Alboran Diapir during the subsidence of the Alboran Basin (Weijermars 1985a,b). The Oligocene nappes were also refolded into a Neogene basin and range structure during their uplift (Weijermars *et al.* 1985).

Dextral displacements on the Crevillente Fault translated the Internal or Betic Zone relative to the External Zone by 250 km mainly between 20 and 5 Ma ago (Hermes 1978, De Smet 1984b). Compilation of the geology of the eastern Betic Zone has revealed that major strike–slip faults, presumably interrelated, also occur in this region: the Palomares Shear Zone, the Almería Fault Zone and the Alhama de Murcia Fault. All these faults still seem active, suggesting that the motion of the Crevillente Fault may still continue.

The Palomares Shear Zone affected a rock volume 44 km wide and at least 80 km long and 30 km deep. It is postulated that the formation of its surface strain pattern was largely controlled by dislocation creep at depth and involved three major stages.

(1) Initiation of the Palomares Fault in an orientation determined by the regional stress pattern between 8 and 15 Ma ago.

(2) Progressive flow softening on the Palomares Fault proper, possibly by further geometric softening at the surface (e.g. formation of shear band cleavage) compensated by structural softening due to dynamic recrystallisation in mylonites at depth.

(3) Formation and progressive widening of the Palomares Shear Zone by shear heating accompanied by strain-rate softening.

The Palomares Fault in the core of the Palomares Shear Zone moved at a mean tensor shear strain rate of 10^{-12} s^{-1} and at a mean shear rate of 2 mm a^{-1}. The relative rigidity of the walls of the Palomares Shear Zone implies strain rates below 10^{-17} s^{-1} since strains caused by such slow strain rates would all remain invisible on the time scale considered here. The range of strain rates within the Palomares Shear Zone has been used to estimate vertically averaged effective viscosities for the crust whilst assuming a constant deviatoric stress level of 100 MPa considered typical for tectonic deformations. The viscosity would be 10^{20} Pa s at the site of the Palomares Fault proper and larger than 10^{25} Pa s outside and at the boundaries of the Palomares Shear Zone. Mechanisms responsible for the flow softening in the Palomares Shear Zone may include geometric, structural, thermal and strain-rate softening.

Some features of the Palomares Fault not yet investigated in the field are predicted here. These are given below.

(1) An eastward dip, as this could potentially explain the asymmetry of the surface strain pattern across the Palomares Shear Zone by asymmetric thermal softening. The modern heat flow at the surface above the east wall of the Palomares Fault may still be larger than that of its west wall (Fig. 11b).

(2) The occurrence of shear band cleavage (and perhaps *C*-fabrics) near the surface (geometric softening) and mylonites at depth (structural softening), as this could explain the anomalously high strains and strain rates on the Palomares Fault.

(3) The occurrence of pseudotachylites, formed by the unsteady motions of the Palomares Fault that caused earthquakes.

Such predictions are considered useful since they may contribute to stimulate research focused on the mechanical processes operating during shear zone formation.

Acknowledgements—I thank the following members of the University of Amsterdam: Drs Th. B. Roep for many clarifying discussions on the geology of the Neogene basins of SE Spain and Professors Emeriti J. J. Hermes and W. P. de Roever for general discussions on the tectonic evolution of SE Spain. I also thank Dr O. J. Simon (Amsterdam) for introducing me to the intricacies of the Betic Cordillera and Dr J. P. Platt (Oxford) for supervision of my 4 months of M.Sc. field mapping in 1979. Dr. A. Allen of the University of Cork (Ireland) is thanked for advice on shear zone motions and critical comments on the original manuscript and also Professor C. J. Talbot and Miss K. Gløersen for criticising and typing, respectively, various later versions in Uppsala. Final draftwork of Figs. 7, 10 and 11 was kindly done by Mrs C. Werström. All other drafts were completed by the author. The final manuscript was prepared after detailed comments of Drs. J. H. Behrmann, J. C. Bousquet and S. H. Treagus during JSG's review procedure. My work was made possible by a postgraduate teaching assistantship at the University of Amsterdam between 1981 and 1983 and grants of the Swedish Natural Science Research Council (NFR) since 1983.

REFERENCES

Akkerman, J. H., Maier, G. & Simon, O. J. 1980. On the geology of the Alpujarride Complex in the western Sierra de las Estancias. *Geologie Mijnb.* **59**, 363–374.

Araña, V. & Vegas, R. 1974. Plate tectonics and volcanism in the Gibraltar Arc. *Tectonophysics* **24**, 197–212.

Azéma, J. 1977. Etude géologique des zones externes des Cordillères Bétiques aux confins des provinces d'Alicante et de Murcie (Espagne). Ph.D. Thesis, University Pierre et Marie Curie, Paris.

Baena, J., Fernandez Vargas, E., García Rodriguez, J. J. & Greene, H. G. 1977. Active faulting in coastal Almería (SE Spain) and adjacent continental shelf. *Seminars Tect. Global*, Fund. Gómez Pardo, Madrid, 1–16.

Banda, E. & Ansorge, J. 1980. Crustal structure under the central and eastern part of the Betic Cordillera. *Geophys. J. R. astr. Soc.* **63**, 515–532.

Banda, E., Udias, A., Mueller, St., Mezcua, J., Boloix, M., Gallart, J. & Aparacio, A. 1983. Crustal structure beneath Spain from deep seismic sounding experiments. *Phys. Earth & Planet. Interiors* **31**, 277–280.

Beaumont, C. 1978. The evolution of sedimentary basins on a viscoelastic lithosphere. *Geophys. J. R. astr. Soc.* **55**, 471–497.

Bellon, H. 1976. Séries magmatiques néogènes et quaternaires du pourtour de la Méditerannée occidentale, comparées dans leur cadre géochronométrique-implications géodynamiques. Ph.D. Thesis, University Paris-Sud (Centre d'Orsay).

Bellon, H. & Brousse, R. 1977. Le magmatisme périméditeranéen occidental. Essai de synthèse. *Bull. Soc. géol. Fr.* **19**, 469–480.

Bellon, H., Bordet, P. & Montenat, C. 1983. Chronologie du magmatisme néogène des Cordillères bétiques (Espagne méridionale). *Bull. Soc. géol. Fr.* **25**, 205–217.

Bonini, W. E., Loomis, T. P. & Robertson, J. D. 1973. Gravity anomalies, ultramafic intrusions, and the tectonics of the region around the Straits of Gibraltar. *J. geophys. Res.* **78**, 1372–1383.

Bott, M. H. P. & Kuznir, N. J. 1984. The origin of tectonic stress in the lithosphere. *Tectonophysics* **105**, 1–13.

Bousquet, J.-C. 1979. Quaternary strike–slip faults in southeastern Spain. *Tectonophysics* **52**, 277–286.

Bousquet, J.-C. & Montenat, C. 1974. Présence de décrochements nord-est–sud-ouest plio-quaternaires, dans les Cordillères bétiques orientales (Espagne). Extension et signification générale. *C. r. Acad. Sci. Paris* **278**, 2617–2620.

Bousquet, J.-C. & Philip, H. 1976a. Observations tectoniques et microtectoniques sur la distension plio-pleistocene ancien dans l'est des Cordillères bétiques (Espagne Méridionale). *Cuad. Géol.* **7**, 57–67.

Bousquet, J.-C. & Philip, H. 1976b. Observations microtectoniques sur la compression nord-sud quaternaire des Cordillères bétiques

orientales (Espagne Méridionale–Arc de Gibraltar). *Bull. Soc. géol. Fr.* **18**, 711–724.
Bousquet, J.-C., Dumas, B. & Montenat, C. 1975. Le décrochement de Palomares: décrochement quaternaire sénèstre du basin de Vera (Cordillères bétiques orientales, Espagne). *Cuad. Géol.* **6**, 113–119.
Brun, J. P. & Cobbold, P. R. 1980. Strain heating and thermal softening in continental shear zones: A review. *J. Struct. Geol.* **2**, 149–158.
Coward, M. P. 1980. Shear zones in the Precambrian crust of southern Africa. *J. Struct. Geol.* **2**, 19–27.
Dabrio, C. J., Esteban, M. & Martin, J. M. 1981. The coral reef of Nijar, Messinian (uppermost Miocene), Almería province, SE Spain. *J. Sed. Petrol.* **51**, 51, 521–539.
De Smet, M. E. M. 1984a. Origin of the Crevillente Fault Zone (Betic Cordilleras, southern Spain). Ph.D. Thesis, Free University of Amsterdam, Free University Press, Amsterdam.
De Smet, M. E. M. 1984b. Wrenching in the external zone of the Betic Cordilleras, southern Spain. *Tectonophysics* **107**, 57–79.
Dronkert, H. 1976. Late Miocene evaporites in the Sorbas Basin and adjoining areas. *Mem. Soc. Geol. Ital.* **16**, 341–362.
Egeler, C. G. & Simon, O. J. 1969a. Sur la tectonique de la Zone Bétique (Cordillères Bétiques, Espagne). *Verh. K. Ned. Akad. Wetensch.* **25**, 1–90.
Egeler, C. G. & Simon, O. J. 1969b. Orogenic evolution of the Betic Zone (Betic Cordilleras, Spain), with emphasis on the nappe structures. *Geologie Mijnb.* **48**, 296–305.
England, P. & Houseman, G. 1985. Rôle of lithospheric strength heterogeneities in the tectonics of Tibet and neighbouring regions. *Nature, Lond.* **315**, 297–301.
Fernex, F. 1964. Sur le jeu de la tectonique postérieure aux nappes dans c'est des zones bétiques. *Arch. Sci. Genève* **17**, 39–46.
Fleitout, L. & Froideavaux, C. 1980. Thermal and mechanical evolution of shear zones. *J. Struct. Geol.* **2**, 159–164.
Foucault, A. 1971. Etude géologique des environs des sources du Guadalquivir (prov. de Jaén et de Grenade, Espagne méridionale). Thesis, University of Paris, Paris.
Geerlings, L. P., Dronkert, H., Van der Poel, H. M. & Van Hinte, J. E. 1980. Chara sp. in Miocene–Pliocene marls at Cuevas del Almanzora, Vera-basin, SE Spain. *Paleontology-Proc.* **83**, 29–37.
Girod, M. & Girod, N. 1977. Contribution de la pétrologie à la connaissance de l'evolution de la Méditerranée occidentale depuis l'Oligocène. *Bull. Soc. géol. Fr.* **19**, 481–488.
Greene, H. G., Snavely, D. & Lucena, J. C. 1977. Neogene tectonics of the Gulf of Almería, Almería Province, Spain. *Messinian Seminars* No. **3**, *Abstr. Congr.* Malaga 26 and 27 Sept. 1977.
Guayau, F., Bayer, R., Bousquet, J.-C., Lachaud, J.-C., Lesquer, A. & Montenat, C. 1977. Le prolongement de l'accident d'Alhama de Murcia entre Murcia et Alicante (Espagne méridionale). *Bull. Soc. géol. Fr.* **19**, 623–629.
Hermes, J. J. 1978. The Stratigraphy of the Subbetic and Southern Prebetic of the Velez Rubio-Caravaca area and its bearing on transcurrent faulting in the Betic Cordilleras of Southern Spain. *Proc. K. Ned. Akad. Wetensch.* **81**, 41–72.
Hermes, J. J. 1984. New data from the Velez Rubío Corridor: support for the transcurrent nature of this linear structure. *Proc. K. Ned. Akad. Wetensch.* series B, **87**, 319–333.
Hernandez Pacheco, A. & Ibarrola, E. 1970. Nuevos datos sobre la petrología y geoquímica de las rocas volcanicas de Alboran (Mediterraneo occidental, Almería). *Estud. Geol.* **26**, 93–103.
Hoedemaeker, P. J. 1973. Olistostromes and other delapsional deposits and their occurrence in the region of Moratella (Prov. de Murcia, Spain). *Scripta Geol.* **19**, 1–207.
Hofman, E. J. 1952. The gravity field of the west-Mediterranean area. *Geologie Mijnb.* **14**, 297–315.
Jacquin, J. P. 1970. Contribution à l'étude géologique et minière de la Sierra de Gadór (Almería Espagne). Ph.D. Thesis, University of Nantes.
Jerez-Mir, L. 1973. Geología de la Zona Prébetica en la transversal de Elche de la Sierra y sectores adyacentes (Províncias de Albacete y Murcia). Thesis, University of Granada.
Kampschuur, W. & Rondeel, H. E. 1975. The origin of the Betic Orogen, Southern Spain. *Tectonophysics* **27**, 39–56.
Kaper, J. J. 1981. De geologie van de zuid-oostelijke Sierra de Cabrera. Internal Report, University of Amsterdam.
Kunze, A. W. G. 1980. On the flexural rigidity and effective viscosity of the lithosphere in the Hawaiian Area. *Tectonophysics* **69**, T1–T8.
Le Pichon, X., Pautot, G. & Weill, J. P. 1972. Opening of the Alboran Sea. *Nature Lond.* **236**, 83–85.
Lodder, W. 1966. Gold-Alunite deposits and zonal wall-rock alteration near Rodalquilar, SE Spain. Ph.D. Thesis, University of Amsterdam.
Loomis, T. P. 1975. Tertiary mantle diapirism, orogeny and plate tectonics east of the Strait of Gibraltar. *Am. J. Sci.* **275**, 31–56.
Marillier, F. & Mueller, St. 1985. The western Mediterranean region as an upper-mantle transition zone between two lithospheric plates. *Tectonophysics* **118**, 113–130.
McNutt, M. & Parker, R. L. 1978. Isostasy in Australia and the evolution of the compensation mechanism. *Science* **199**, 773–774.
Means, W. D. 1976. *Stress and Strain*. Springer, New York.
Montenat, C., Reneville, P. & Bizon, G. 1978. Le Néogène des environs d'Aguilas (provinces de Murcia et d'Almería), Cordillères Bétiques, Espagne. *Mus. Natl Hist. Nat. (Paris)* 3e Sér. **511**, 37–54.
Mulder, C. J. 1973. Tectonic framework and distribution of Miocene evaporites in the Mediterranean. *Messinian Events in the Mediterranean* (edited by Drooger, C.). North-Holland, Amsterdam, 44–59.
Mulder, C. J. & Parry, G. R. 1977. Late Tertiary evolution of the Alboran Sea at the eastern entrance of the Strait of Gibraltar. *Int. Symp. Structural Evolution of the Mediterranean Basins*, Split, Editions Techn., Paris, 401–410.
Neugebauer, H. J. 1983. Mechanical aspects of continental rifting. *Tectonophysics* **94**, 91–108.
Nobel, F. A., Andriessen, P. A. M., Hebeda, E. H., Priem, H. N. A. & Rondeel, H. E. 1981. Isotopic dating of the post-Alpine Neogene volcanism in the Betic Cordilleras, southern Spain. *Geologie Mijnb.* **60**, 209–214.
Pagnier, H. 1976. Depth of deposition of Messinian selenitic gypsum in the basin of Sorbas (SE Spain). *Mem. Soc. Geol. Ital.* **16**, 363–367.
Pfiffner, O. A. & Ramsay, J. G. 1982. Constraints on geological strain rates: Arguments from finite strain states of naturally deformed rocks. *J. geophys. Res.* **87**, 311–321.
Pineda Velasco, A. 1984. Las mineralizaciones metálicas y su context geológico en el área volcánica neógena del Cabo de Gata (Almería, SE de Espana). *Bol. Geol. y Minero* **95/96**, 569–592.
Platt, J. P. & Behrmann, J. H. 1986. Structures and fabrics in a crustal-scale shear zone, Betic Cordillera, SE Spain. *J. Struct. Geol.* **8**, 15–33.
Platt, J. P., Van den Eeckhout, B., Janzen, E., Konert, G., Simon, O. J. & Weijermars, R. 1983. The structure and tectonic evolution of the Aguilón fold-nappe, Sierra Alhamilla, Betic Cordilleras, SE Spain. *J. Struct. Geol.* **5**, 519–538.
Poirier, J. P, 1980. Shear localization and shear instability in materials in the ductile field. *J. Struct. Geol.* **2**, 135–142.
Poirier, J. P, 1985. *Creep of Crystals*. Cambridge University Press, Cambridge.
Postma, G. 1984a. Slumps and their deposits in fan delta and slope. *Geology* **12**, 27–30.
Postma, G. 1984b. Mass-flow conglomerates in a submarine canyon: Abrioja fan-delta, Pliocene, southeast Spain. In: *Sedimentology of Gravels and Conglomerates* (edited by Koster, E. H. & Steel, R. J.), *Can. Soc. Petr. Geol. Mem.* **10**, 237–258.
Ramsay, J. G. 1980. Shear zone geometry: a review. *J. Struct. Geol.* **2**, 83–99.
Ramsay, J. G. & Graham, R. H. 1970. Strain variation in shear belts. *Can. J. Earth Sci.* **7**, 786–813.
Ramsay, J. G. & Huber, M. I. K. 1983. *The Techniques of Modern Structural Geology. Volume 1: Strain Analysis*. Academic Press, London, 1–307.
Roep, Th. B., Beets, D. J., Dronkert, H. & Pagnier, H. 1978. A pro-grading coastal sequence of wave-built structures of Messinian age, Sorbas, Almería, Spain. *Sediment. Geol.* **22**, 135–163.
Rondeel, H. E. 1965. Geological investigations in the western Sierra Cabrera and adjoining area, southeastern Spain. Ph.D. Thesis, University of Amsterdam.
Rondeel, H. E., Weijermars, R. & van Dorssen, H. G. 1984. Re-activation of early reverse faults associated with oblique strike–slip faulting: a mechanism for crustal shortening (Macizo de Nevera, Sierra de Albarracín, Spain). *Geologie Mijnb.* **63**, 387–398.
Rutter, E. H. 1986. On the nomenclature of mode of failure transitions in rocks. *Tectonophysics* **122**, 381–387.
Seilacher, A. 1984. Sedimentary structures tentatively attributed to seismic events. *Mar. Geol.* **35**, 1–12.
Sibson, R. H. 1980. Transient discontinuities in ductile shear zones. *J. Struct. Geol.* **2**, 165–171.
Simpson, C. 1983. Displacement and strain patterns from naturally occurring shear zone terminations. *J. Struct. Geol.* **5**, 497–506.
Sleep, N. H. & Snell, N. S. 1976. Thermal contraction and flexure of mid-continent and Atlantic marginal basins. *Geophys. J. R. astr. Soc.* **45**, 125–154.

Stanley, D. J., Gehin, C. E. & Bartolini, C. 1970. Flysch-type sedimentation in the Alboran Sea, western Mediterranean. *Nature, Lond.* **288**, 979–983.
Torres-Roldán, R. 1979. The tectonic subdivision of the Betic Zone (Betic Cordilleras, southern Spain): its significance and one possible geotectonic scenario for the westernmost Alpine belt. *Am. J. Sci.* **279**, 19–51.
Turcotte, D. L. & Schubert, G. 1982. *Geodynamics*. Wiley, New York.
Van Bemmelen, R. W. 1952. Gravity Field and Orogenesis in the West Mediterranean Sea. *Geologie Mijnb.* **14**, 306–315.
Van Bemmelen, R. W. 1969. Origin of the western Mediterranean Sea. *Verh. K. Ned. geol. mijnbouwkd. Genoot* **26**, 13–52.
Van Bemmelen, R. W. 1973. Geodynamic models for the Alpine type of orogeny (test-case II: the Alps in central-Europe). *Tectonophysics* **18**, 33–79.
Van de Fliert, J. R., Graven, H., Hermes, J. J. & De Smet, M. E. M. 1980. On stratigraphic anomalies associated with major transcurrent faulting. *Eclog. geol. Helv.* **73**, 223–237.
Veeken, P. C. H. 1983. Stratigraphy of the Neogene-Quaternary Pulpi Basin, Provinces Murcia and Almería (SE Spain). *Geologie Mijnb.* **62**, 255–265.
Vissers, R. L. M. 1981. A structural study of the central Sierra de los Filabres (Betic Zone, SE Spain), with emphasis on deformational processes and their relation to the Alpine metamorphism. *GUA papers of Geology* 15, University of Amsterdam.
Völk, H. R. 1966. Aggradational directions and biofacies in the youngest postorogenic deposits of southeastern Spain. A contribution to the determination of the age of the East Mediterranean Coast of Spain. *Palaeogeogr. Palaeoclimatol. Palaeoecol.* **2**, 313–331.
Völk, H. R. 1967. Zur geologie und stratigraphie des Neogenbeckens von Vera, Südost-Spanien. Ph.D. Thesis, University of Amsterdam.
Völk, H. R. & Rondeel, H. E. 1964. Zur Gliederung des Jungstertiärs in Becken von Vera, Südost-Spanien. *Geologie Mijnb.* **43**, 310–315.
Weijermars, R. 1985a. In search for a relationship between harmonic resolutions of the geoid, convective stress patterns and tectonics in the lithosphere: A possible explanation for the Betic-Rif orocline. *Phys. Earth & Planet. Interiors* **37**, 135–148.
Weijermars, R. 1985b. Uplift and subsidence history of the Alboran Basin and a profile of the Alboran Diapir. *Geologie Mijnb.* **64**, 349–356.
Weijermars, R. 1985c. Directional variations of fold axes in progressive deformation, an example from a Betic fold nappe in S. Spain. *Geologie Mijnb.* **64**, 271–280.
Weijermars, R. & Rondeel, H. E. 1984. Shear band foliation as an indicator of sense of shear: Field observations in central Spain. *Geology* **12**, 603–606.
Weijermars, R. & Schmeling, H. 1986. Scaling of Newtonian and non-Newtonian fluid dynamics without inertia for quantitative modelling of rock flow due to gravity (including the concept of rheological similarity). *Phys. Earth & Planet. Interiors* **43**, 316–330.
Weijermars, R., Roep, Th. B., Van den Eeckhout, B., Postma, G. & Kleverlaan, K. 1985. Uplift history of a Betic fold nappe inferred from Neogene–Quaternary sedimentation and tectonics (in the Sierra Alhamilla and Almería, Sorbas and Tabernas Basins of the Betic Cordilleras, SE Spain). *Geologie Mijnb.* **64**, 397–411.
Westra, G. 1969. Petrogenesis of a composite metamorphic facies series in an intricate fault-zone in the southeastern Sierra Cabrare, SE Spain. Ph.D. Thesis, University of Amsterdam.
Zeck, H. P. 1970. An erupted migmatite from Cerro el Hoyazo (SE Spain). *Contr. Miner. Petrol.* **26**, 225–246.